Effects of Ion Size and Valence on Ion Distribution in Mixed Counterion Systems of a Rodlike Polyelectrolyte Solution. 2. Mixed-Valence Counterion Systems†

Takuhiro Nishio and Akira Minakata*

Department of Physics, Hamamatsu University School of Medicine, Hamamatsu 431-3192, Japan

Received: December 5, 2002; In Final Form: February 24, 2003

The characteristics of the ion distributions are investigated in the systems of salt-free polyelectrolyte solution with mixed-valence counterions using a cylindrical cell model. The mixtures of two species of the counterion having different valences are simulated systematically by means of the Monte Carlo method in a primitive model of the rodlike polyelectrolyte solution. The comparisons of the free fractions and the selectivity coefficients by this method are performed with the numerical solutions of the Poisson−Boltzmann equation. A significant accumulation of the multivalent counterions found in the Monte Carlo simulations is examined under various conditions. The differences between both methods and additional effects of ion size are discussed in terms of the relation to the simple counterion condensation theory and the effect of ion−ion correlations.

Introduction

The size and valence of counterions are important parameters in the elucidation of the solution properties of the polyelectrolyte. The ion distribution in the mixed counterion system with a different size and/or valence is characterized by the interactions between the polyion and the mobile ions. Following the preceding paper,[1] the counterion distribution and ion selectivity in the mixed-valence system are examined for the salt-free solutions of the rodlike polyelectrolyte.

In the mixed-valence system, the fact is notable that the counterions of higher valence are accumulated preferentially in the vicinity of the polyion and that the counterions of lower valence are pushed farther away from the polyion. This valence selectivity is qualitatively demonstrated in terms of the simple two-phase approximation on the salt-free mixed-valence system.[2] It is also supported by the counterion condensation hypothesis by Manning applied to the counterion mixture.[3,4]

The general analysis of the Poisson−Boltzmann (PB) equation for the valence selectivity was presented in the limit of infinite dilution.[5] Various numerical studies of the PB theory had been made for the mixed-valence salt system in the rodlike polyelectrolyte solution to interpret the competitive interaction of the counterions.[6−10] Colligative properties in the mixed-valence counterion system were interpreted semiquantitatively by the numerical solution of the PB equation. The PB approach has also been regarded as advantageous to the analysis of the competitive binding of the charged ligands to the polyelectrolyte.[11,12]

The Monte Carlo (MC) simulation revealed, however, a stronger accumulation of multivalent counterions than in the PB calculation for the simple model of DNA solution.[13] This tendency in the mixed-valence salt system was investigated in subsequent studies by the MC calculation.[14−16] These results indicate the insufficiency of the classical PB equation by neglecting the effects of ion−ion correlation and finite ion size. The theoretical approaches by the hypernetted chain (HNC) approximation or the modified Poisson−Boltzmann (MPB) equation were examined to interpret this discrepancy.[14,17,18] Recently, the multivalent cation distributions in the vicinity of DNA and their competition with a monovalent cation were investigated in more detail by the simulations.[19−23]

The present study is carried out to examine the influences of ion size and valence through the canonical MC simulations for the mixed counterion systems of a rodlike polyelectrolyte solution. The main purpose is to clarify the limitation of the PB method by using the MC simulation under the same condition (i.e., the smeared charged rod with finite-sized counterions). In this article, the results of the mixtures of two counterion species with different valences are presented for the cylindrical cell system without salt. This valence selectivity and its dependence on several parameters are obtained by MC simulations.

The valence selectivity is more significant than the size selectivity under usual conditions, even in the theoretical framework of the PB equation. The accumulation of the counterion with higher valence is strengthened in the MC system as a consequence of the ion−ion correlations, as presented in the preceding paper. Then, the deviation of the MC result from the PB result is quite evident in the valence selectivity because of the strong correlations between the mobile multivalent ions.

The aim of this work is to examine the effects of ion−ion correlation in multivalent ions and finite ion size in the mixed-valence system in salt-free solutions when the effect of a co-ion is excluded. In some cases, systems containing ions with a fractional valence are employed to obtain the overall tendency by changing parameters as well as to understand the difference between the MC and PB results, although the assumption of the fractional valence is rather unrealistic. The systematic investigation of the accumulation of counterions with higher valence seems to be effective in clarifying the properties of the pronounced valence selectivity in the biological systems. The present study provides some fundamental features of the ion−ion correlation in the primitive model even within the framework of the isolated cell system.

Method

A. Monte Carlo Simulation and Poisson−Boltzmann Equation. The systems of mixed-valence counterions without

† Part of the special issue "International Symposium on Polyelectrolytes".

* Corresponding author. E-mail: aminak@nifty.com.

10.1021/jp022531a CCC: $25.00
Published on Web 06/05/2003

added salt are presented here to clarify their influences on the ion distributions. A polyion is assumed to be a simple rod with uniformly smeared charge in the continuum dielectric system, and the mobile counterions are treated as finite-sized spheres with a hard-core potential. The radial counterion distributions are evaluated around the polyion in a cylindrical cell in the canonical MC simulations with high accuracy. Numerical analysis for the differential equation is applied to solve the PB equations.

In the infinitely long cylindrical cell with radius R, a polymer rod with radius a is assumed to be at the center of the cell. The mixture of two species (A and B) of spherical mobile counterions with different positive valence is considered in the continuum dielectric medium. The negative charge is assumed to be smeared uniformly on the surface of the polymer cylinder. The value, b, is defined as the mean distance of an elementary charge along the polymer axis. The radii and valences of counterions A and B are defined as σ_A, σ_B and z_A, z_B, respectively. The definitions are adopted such that $l_B = e^2/(4\pi\epsilon_0 D k_B T)$ is the Bjerrum length, where e is the elementary protonic charge, k_B is the Boltzmann constant, T is the absolute temperature, ϵ_0 is the permittivity of the vacuum, and D is the relative dielectric constant of the solvent water.

The equivalent molar concentration of the polyion, C_P, is defined as

$$C_P = \frac{1}{1000 N_{AV}} \frac{1}{\pi R^2 b} = \frac{1}{1000 N_{AV}} \frac{\xi}{\pi R^2 l_B} \quad (1)$$

where N_{AV} is Avogadro's constant and $\xi = e^2/(4\pi\epsilon_0 D b k_B T) = l_B/b$ is the charge-density parameter. The electroneutrality condition is presented as

$$C_P = z_A \bar{C}_A + z_B \bar{C}_B \quad (2)$$

where $\bar{C}_A$ and $\bar{C}_B$ are the mean molar concentrations of counterions A and B in the cell volume, respectively. The unit of molar concentration C is given in mol/dm^3.

By the MC simulation and the numerical PB calculation in the salt-free system, the counterion concentration $C(r)$ is evaluated at the radial distance from the cell axis, r. These practical procedures were described in the preceding paper.[1]

In the present MC work, long iterations ($\geq 32 \times 10^5$ Monte Carlo steps per ion) are necessary in many cases to depress the mean error of the concentration at a cell boundary. The acceptance ratio in each MC run is settled within the range 0.43−0.57 by the regulation of the step width of the movement trial. In most cases, the polyion with 200 electronic charges is adopted in the central cell. For the dilute solutions, the long cell containing 400 polyion charges is needed to obtain a more reliable MC result. When reliable data cannot be obtained, the data is discarded.

Although an analytical solution is not known for the PB equation in the case of a mixed-valence system without salt, the following general relation is confirmed in the present PB calculations with high accuracy,[5]

$$\frac{\xi}{2} C_P = \frac{1}{R^2} \sum_i (a + \sigma_i)^2 C_i(a + \sigma_i) - \sum_i C_i(R) + \sum_i \bar{C}_i \quad (3)$$

where $C_i(r)$ and $\bar{C}_i$ are the local concentrations at r and the mean concentration of ion species i, respectively. σ_i is the radius of each mobile ion.

B. Representation of Results and Parameters. The mixtures of multivalent and monovalent counterions of the same size or of different sizes are examined under conditions that are similar to those given in the preceding paper. The dependences of the ion distribution on the linear charge density ξ, fraction of ion mixture w, polyion concentration C_P, polyion radius a, ion valence z, and hydrated ion radius σ are investigated in the mixture of counterions with different valences. The equivalent fraction of ion A is defined as

$$w_A = \frac{z_A \bar{C}_A}{z_A \bar{C}_A + z_B \bar{C}_B} \quad (4)$$

To represent the accumulation of the ions, the ratios of the ion concentration at the outer cell boundary to the mean concentration are evaluated as a "free fraction"

$$f_A = \frac{C_A(R)}{\bar{C}_A} \qquad f_B = \frac{C_B(R)}{\bar{C}_B} \quad (5)$$

To show the ion selectivity, the selectivity coefficient is adopted for simplicity according to the preceding paper. The selectivity coefficient of ion A against ion B is given as follows:[24]

$$K_{A,B} = \frac{\bar{C}_A}{\bar{C}_B} \frac{C_B(R)}{C_A(R)} = \frac{f_B}{f_A} \quad (6)$$

This coefficient is sensitive enough to detect the ion selectivity in salt-free systems.

The temperature applied in the calculations is 25 °C, and the Bjerrum length is taken as 7.135 Å in all cases. The conditions of the solution system are chosen by considering mainly the feasibility of the precise MC simulation.

Results and Discussion

A. Dependence on Charge-Density Parameter and Counterion Valence. First, the dependences on the charge density of the polyion are examined for four combinations of the mixed-valence counterions ($z_A = 1$, 2, 3 and 4; $z_B = z_A/2$) with the same size ($\sigma_A = \sigma_B = 3.0$ Å). The dependence of the free fractions f_A and f_B and the selectivity coefficient $K_{A,B}$ on the value $z_A\xi$ is shown at $w_A = 0.75$ in Figure 1. The values in the same cell are common functions of $z_A\xi$ in the framework of the PB equation in salt-free systems. In the Figure, the MC results are presented together with the PB solution in the case of $a = 5.0$ Å and $R = 172.0$ Å, corresponding to $C_P = 2.5041 \times 10^{-3}$ mol equiv/dm^3 at $\xi = 1$. Here, C_P is proportional to ξ.

The MC results of f_A and $K_{A,B}$ are more pronounced than those of the PB solutions with increasing charge density, that is, f_A decreases more steeply and $K_{A,B}$ increases more sharply. This tendency is clearly demonstrated by introducing fractional valences. The deviation of f_A and $K_{A,B}$ is emphasized when ion A is multivalent.

Above a critical point of the counterion condensation hypothesis, $z_A\xi = 1$, and the deviation of f_A and $K_{A,B}$ begins to spread in the cases of $z_A \geq 2$. The MC curves of log $K_{A,B}$ increase almost linearly in the plot although the PB curve is slightly above another critical point, $z_A\xi = 4$, of the theory (see below). Thus, considerable deviations are observed for $z_A\xi \geq 4$. The MC result in the case of $z_A = 2$ is close to the PB result even at $z_A\xi = 3$. However, the deviation in this case also becomes remarkable for $z_A\xi \geq 4$. On the contrary, the MC results of f_B are almost equal to one another and relatively close to the PB solutions (within ±8%) over the whole range in all

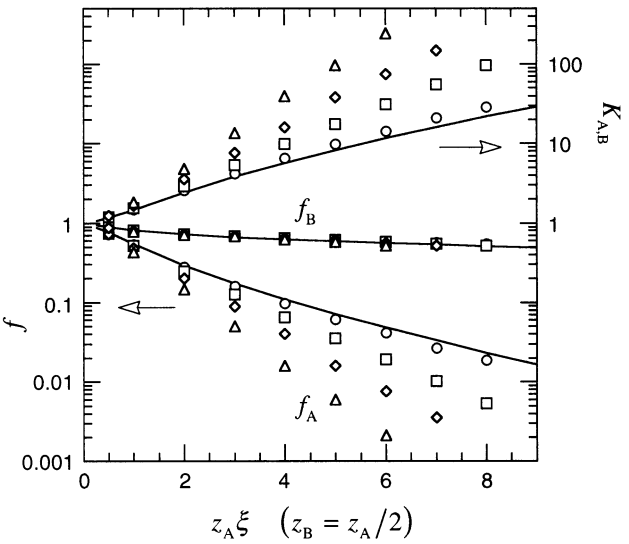

Figure 1. Dependence of the free fractions f_A and f_B (lower data, left axis) and of the selectivity coefficient $K_{A,B}$ (upper data, right axis) on the polyion charge-density parameter ξ in the mixture of two counterion species with different valences and the same size ($\sigma_A = \sigma_B = \sigma =$ 3.0 Å) for combinations of the counterion valence ($z_A = 1$, 2, 3, and 4; $z_B = z_A/2$) at $w_A = 0.75$. The abscissa is plotted against the product of counterion valence z_A and the polyion charge density parameter ξ. The MC results for $z_A = 1$ (○), 2 (□), 3 (◇), and 4 (△) are presented together with the PB solution (—) in the case of $a = 5.0$ Å and $R = 172.0$ Å [$(a + \sigma)/R = 0.04651$]. Lower symbols, f_A; middle symbols, f_B; and upper symbols, $K_{A,B}$.

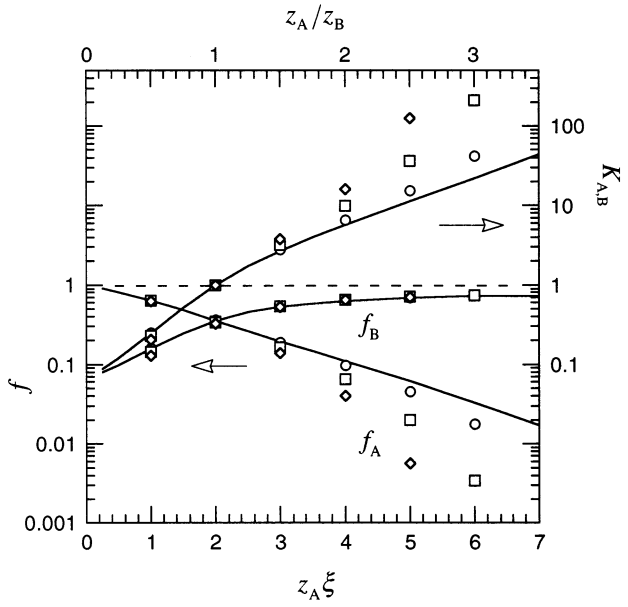

Figure 2. Dependence of the free fractions f_A and f_B and of the selectivity coefficient $K_{A,B}$ on the valence of ion A, z_A, in the case of the fixed $z_B\xi = 2$ at $w_A = 0.75$. The abscissa is plotted by the value $z_A\xi$. The upper abscissa indicates the ratio z_A/z_B. The MC results for $z_B = 0.5$ ($\xi = 4$, ○), 1 ($\xi = 2$, □), and 1.5 ($\xi = {}^4/_3$, ◇) are presented together with the common PB solution (—). The dashed line represents $K_{A,B} = 1$. Other details are the same as in Figure 1.

valence combinations. The mutual coincidence of f_B indicates that the introduction of fractional valence for z_B does not provide any artificial problems. The deviations of the selectivity coefficient of the MC results from the PB solutions reflect the deviations of f_A.

Next, the dependence of the valence of ion A is examined when the valence of ion B and the charge density are fixed. The dependence on $z_A\xi$ is presented in the cases of $z_B\xi = 2$ ($z_B = 0.5$ at $\xi = 4$, $z_B = 1$ at $\xi = 2$, and $z_B = 1.5$ at $\xi = {}^4/_3$) and w_A to be fixed at 0.75 in Figure 2 under the same conditions of the cell and ion sizes in Figure 1.

When the value of $z_A\xi$ is lower than 3, the deviation of the MC results from the PB solution is very small. For $z_A\xi \geq 4$, the MC results of the free fraction of ion A and the selectivity coefficient deviate from the PB results. The free fraction of ion B by the MC method is in agreement with the PB results over the whole range. A very sharp increase in the selectivity of the multivalent counterion is indicated in the higher range.

Oosawa analyzed the dependence of the charge density in the mixed-valence system without salt. The essence is represented using the present notation in the case of $z_A > z_B$ as follows:[2]

(a) $0 \leq \xi \leq 1/z_A$
ions A and B, not condensed

(b) $1/z_A \leq \xi \leq 1/[z_A(1 - w_A)]$
ion A, partially condensed; ion B, not condensed

(c) $1/[z_A(1 - w_A)] \leq \xi \leq 1/[z_B(1 - w_A)]$
ion A, fully condensed; ion B, not condensed

(d) $1/[z_B(1 - w_A)] \leq \xi$
ion A, fully condensed; ion B, partially condensed

(7)

The conclusion of the counterion condensation was proposed as a "limiting law" in which the radii of the polyion and mobile ions are neglected. The calculations at a finite concentration do not give the transition point. These theoretical descriptions are, however, suggestive of the qualitative illustration of the present results, in particular, of the MC simulation, because the limiting law emphasizes the counterion condensation phenomenon. The deviation of the MC results from the PB results appears near the point where the condensation of ion A occurs (at $z_A\xi = 1/(1 - w_A) = 1$ in Figures 1 and 2). Furthermore, the increase in the deviation is observed above the full condensation point of ion A ($z_A\xi = 4$).

An empirical relation can be extracted for the value of f_A from Figures 1 and 2 if ion A is multivalent, as follows:

$$\ln f_A \propto -z_A^{\alpha}\xi \quad (\alpha = 1.6-1.8) \tag{8}$$

When the data of f_A in Figure 1 is plotted as a function of $z_A^{\alpha}\xi$ ($\alpha = 1.68$), as seen in Figure 3, the values in the case of $z_A \geq 2$ give an almost common line. The values of f_A in the case of $z_A = 1$ deviate from the line. The relation in which the valence is represented as a fractional power law, z_A^{α}, instead of $\alpha = 1$ or 2 suggests the correlation between multivalent counterions as well as the degree of shielding effect of the polyion charge in the neighborhood of the polyion. This means that the effect of valence is not simply understood in terms of the condensation condition determined by parameter $z_A\xi$. Also, it is not the case of ordinary electrochemistry where the ionic strength is proportional to z_A^2. At present, the true meaning of the value $\alpha = 1.68$ is unknown.

In the MC system, the electrostatic repulsion is lowered between the multivalent counterion accumulated near the polyion, relative to the PB approximation. The mutual repulsion of the discrete charges prevents them from getting arbitrarily close together. In this situation, a multivalent counterion accumulates more easily because of its lower entropic cost. The effect of the correlation is small for ions far from the polyion

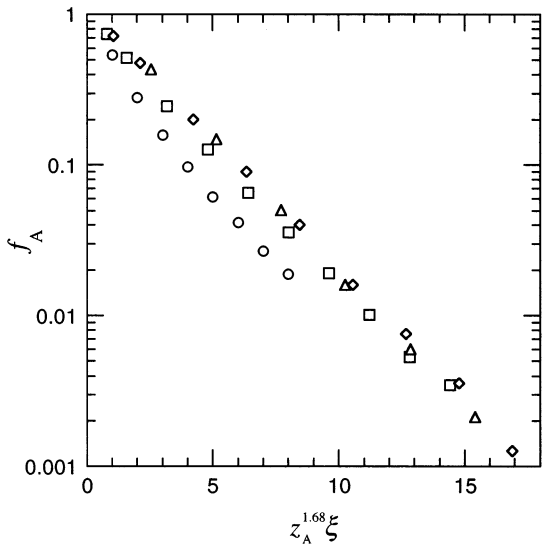

Figure 3. Change in the free fractions f_A from the MC results in Figure 1 as a function of the value $z_A^{1.68}\xi$. The parameters and symbols are the same as in Figure 1.

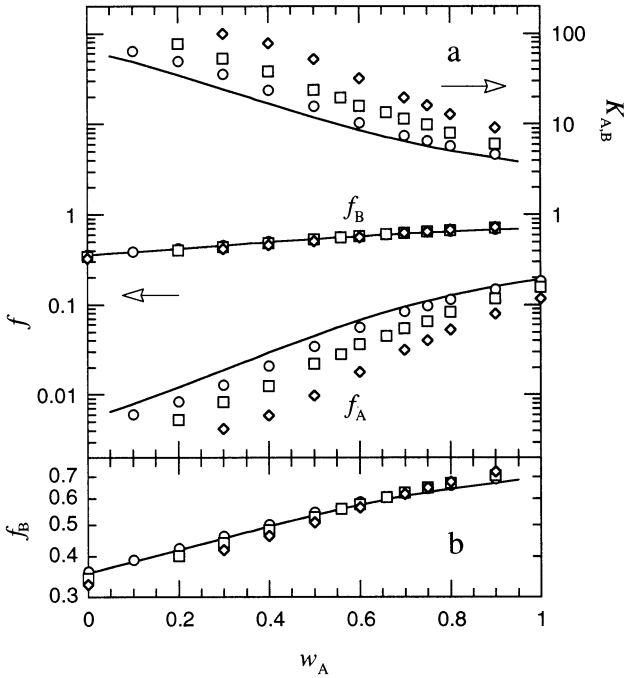

Figure 4. Dependence of the free fractions f_A and f_B and of the selectivity coefficient $K_{A,B}$ (a) and an expanded plot for f_B (b) on the fraction of the ion mixture w_A for the mixed-valence counterion system ($z_B = z_A/2$) at $z_A\xi = 4$. The MC results for $z_A = 1$ ($\xi = 4$, ○), 2 ($\xi = 2$, □), and 3 ($\xi = {}^4/_3$, ◇) are presented together with the PB solution (—). The other parameters of the cell and ions are the same as in Figure 1.

and/or for a polyion with low charge density. Consequently, the MC result gives an increased accumulation of the counterions with higher valence near the polyion surface compared to the PB approximation. In addition, the PB theory cannot explain the difference between the valence combinations.

B. Dependence on Fraction of Ion Mixture. The dependence of f_A, f_B, and $K_{A,B}$ on the fraction of ion A is presented in Figure 4 for the mixtures of the counterions ($z_A = 1$, 2, and 3; $z_B = z_A/2$) at $z_A\xi = 4$ with the same parameters of the cell and ions in Figure 1. The free fraction of the ion with the higher valence decreases with decreasing w_A. In the plot of log f_A and log f_B versus w_A, the slopes are steeper in the lower range of w_A than in the upper range in both the PB and MC results. The change in log f_B is more gradual than that in log f_A.

The deviation of the MC result from the PB solution increases with decreasing w_A for the free fraction of ion A and the selectivity coefficient, especially in the lower w_A range ($w_A \leq 0.65$). The accumulation of the counterion with higher valence in the MC system becomes significant when lowering its fraction in the solution. However, it is difficult to know the behavior of the MC result in the range of $w_A \leq 0.3$. In the case of $z_A = 2$ and 3, the MC results of the free fraction of ion B are lower than the PB results in the range of $w_A \leq 0.5$ and higher in the range of $w_A \geq 0.7$, as shown in Figure 4b. The cross points are at $w_A = 0.56$ in the case of $z_A = 2$ and around $w_A = 0.65$ in the case of $z_A = 3$. The change of the free fraction of the ion with lower valence near the cross point is emphasized in the MC result. This suggests the tendency of accumulation of the ion with lower valence in the lower range and the exclusion by the multivalent ion in the upper range of w_A.

The results of the w_A dependence shown in Figure 4 indicate a strong "binding" of counterion A with higher valence and a replacement of counterion B with ion A. The relations in eq 7 can be rewritten for the range of w_A in the case of $\xi \geq 1/z_A$ as follows:

(a) $0 < w_A \leq 1 - (1/(z_B\xi))$
ion A, fully condensed; ion B, partially condensed

(b) $1 - (1/(z_B\xi)) \leq w_A \leq 1 - (1/(z_A\xi))$
ion A, fully condensed; ion B, not condensed

(c) $1 - (1/(z_A\xi)) \leq w_A < 1$
ion A, partially condensed; ion B, not condensed

(9)

In the above case of $z_B = z_A/2$ at $z_A\xi = 4$, the expected transition point for ion A (fully condensed to partially condensed state) is $w_A = 0.75$, and the transition point for ion B (partially condensed to noncondensed state) is $w_A = 0.5$. In the present calculations of the w_A dependence at finite concentration, one can predict from eq 9 the increase in the deviation of the MC from the PB result, although the critical points are shifted depending on the valence combination and ion sizes.

C. Dependence on Polymer Concentration and Polymer Radius. In the case of $\sigma_A = \sigma_B = \sigma$, the profiles of ion distribution and the selectivity coefficient are determined by the ratio $(a + \sigma)/R$ in the PB system if the charge densities of the polyion and the counterion composition are given. The accumulation of the counterion with higher valence is strengthened when decreasing this ratio. The dependence of the selectivity coefficient on this ratio increases when lowering the equivalent fraction w_A. The deviation of the MC results from the PB results with dilution (decrease in $(a + \sigma)/R$) is valuable in understanding the property of the ion accumulation in the MC system.

Even if the ratio $(a + \sigma)/R$ is fixed, various combinations are possible for the cell radius, the mobile ion size, and the polyion radius in the MC system. In Figure 5, the difference between the variation in cell radius R and the variation in a is represented in the case of $z_A = 2$, $z_B = 1$, and $\xi = 2$ at $w_A = 0.8$. The accumulation of the counterion with higher valence is strengthened more in the MC system than in the PB equation by the thinning of the polymer radius whereas the counterion sizes are fixed. The deviation of the MC result from the PB result decreases with increasing cell radius at this w_A value. In the case of f_B, the MC and PB results are very close.

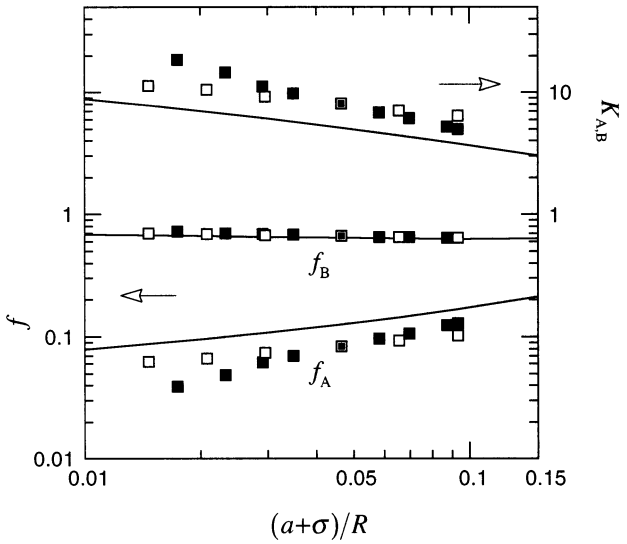

Figure 5. Dependence of the free fractions f_A and f_B and of the selectivity coefficient $K_{A,B}$ ($z_A = 2$, $z_B = 1$) on log $(a + \sigma)/R$ at $w_A = 0.8$ for $\sigma_A = \sigma_B = \sigma = 3$ Å and $\xi = 2$. The MC results in the case of variations in cell radius R at a fixed rod radius $a = 5$ Å (□) and in the case of variations in a at a fixed $R = 172$ Å (■) are presented together with the common PB solution (—). Other details are the same as in Figure 1.

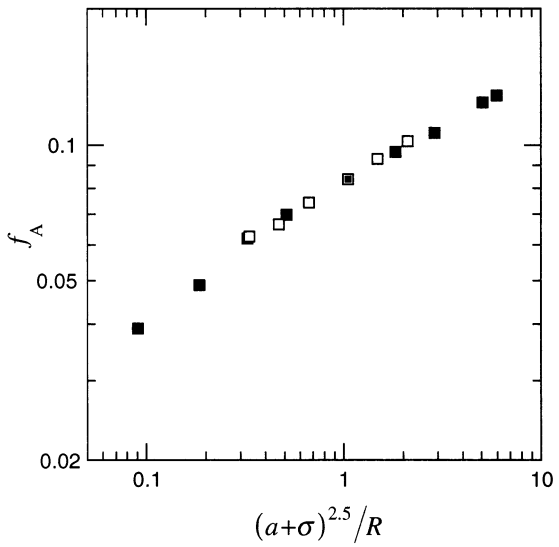

Figure 6. Change in the free fractions f_A from the MC results in Figure 5 as a function of the value $(a + \sigma)^{2.5}/R$. The abscissa is plotted on a logarithmic scale. The parameters and symbols are the same as in Figure 5.

By plotting f_A values versus $(a + \sigma)^{2.5}/R$, both data sets can coincide (Figure 6). Although the meaning of the value 2.5 is unclear, this fact indicates the importance of the interactions in the narrow space near the polyion to the ion selectivity in the MC system.

D. Additional Effects of Differences in Counterion Size. If the ion radius is different between both ion species in the mixed-valence system, then the additional effect of size differences appears as reported in the preceding paper. The effect of the counterion size is examined for the mixtures of divalent (A) and monovalent (B) counterions. In Figure 7, the values of f_A, f_B, and $K_{A,B}$ are plotted against σ_A over a wide range—at $\xi = 2$ in the case of a fixed radius of monovalent ion B $\sigma_B = 3.0$ Å for $w_A = 0.5$ and 0.9. These indicate that the decrease in the accumulation of the divalent ions due to the enlargement results in a slight increase in the accumulation of the monovalent

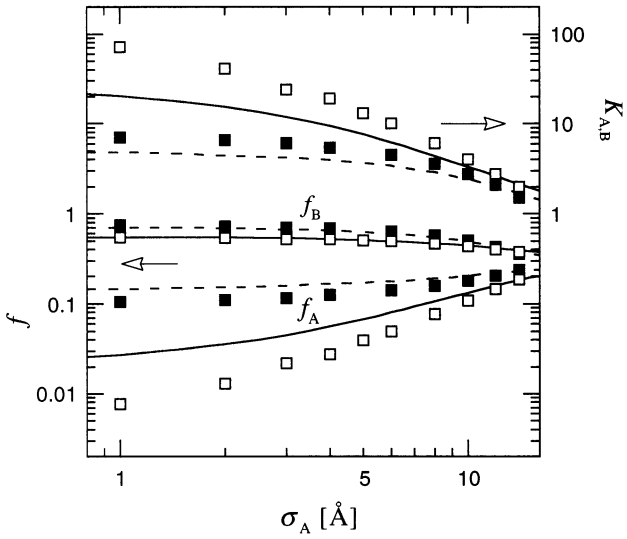

Figure 7. Dependence of the free fractions f_A and f_B and of the selectivity coefficient $K_{A,B}$ on the radius of divalent ion A, σ_A, in the mixture of two counterion species ($z_A = 2$, $z_B = 1$) with a fixed radius of monovalent ion B, $\sigma_B = 3$ Å, $\xi = 2$ at $w_A = 0.5$ (—, □), and $w_A = 0.9$ (- - -, ■). The abscissa is plotted on a logarithmic scale. Other details are the same as in Figure 1.

ions. The σ_A dependences of f_A and $K_{A,B}$ are larger for low w_A, although the dependence of f_B is larger for high w_A.

The change in f_A is larger for the MC result than for the PB result, especially for low w_A. The selectivity coefficient of the MC result is about 3.5-fold the PB solution at $\sigma_A = 1$ Å and $w_A = 0.5$. However, the MC and PB results almost coincide with each other in the σ_A range of 12−14 Å at both w_A values.

The effect of size differences is also significant for low values of w_A. Increases in the core repulsion between the counterions with higher valence can reduce their accumulation tendency in the MC system. The accumulation of the ion with higher valence is strengthened by increasing size of the counterion with lower valence because of the withdrawal of the latter species from the polyion.

Conclusions

The present MC calculations clarify the dependences of the accumulation tendency of the multivalent counterion in the mixed-valence system on the parameters of the cell system. The MC result in the salt-free system gives a considerably strong accumulation of the multivalent counterion compared with that in the PB solution. The tendency is emphasized in the cases of high-charge-density polyions, low fractions of multivalent ions, thin polyion rods, and small multivalent counterions. The dependence of the valence selectivity on solution concentration (cell radius) in the MC results is not larger than that in the PB results.

The accumulation of counterions with higher valence screens the polyion charge. The remaining effective charge density is decreased below a critical value for most counterions with lower valence in the MC system as well as in the PB system. The distribution of ions with lower valence by the MC is relatively close to that by the PB calculation within the limits of small-ion size effects.

The use of the classical counterion condensation hypothesis of the mixed-valence system seems to be practical, to some degree, in predicting the deviations between the MC and PB methods. However, the source of the strong accumulation tendency of the multivalent counterion is the positional cor-

relation between the discrete ions in the vicinity of the polyion. The two-phase approximation in the theory seems to have an effect that is similar to the counterion accumulation obtained in this study.

Acknowledgment. The MC calculations in this study were carried out using the vector processor in the information processing center of Hamamatsu University School of Medicine. The subroutines in Scientific Subroutine Library II (SSLII) by Fujitsu Limited were adopted to solve the ordinary differential equations and so on.

References and Notes

(1) Nishio, T.; Minakata, A. *J. Chem. Phys.* **2000**, *113*, 10784.
(2) Oosawa, F. *Polyelectrolytes*; Marcel Dekker: New York, 1971; Chapter 4.
(3) Manning, G. S. *Q. Rev. Biophys.* **1978**, *11*, 179.
(4) Manning, G. S. *J. Phys. Chem.* **1984**, *88*, 6654.
(5) Ramanathan, G. V. *J. Chem. Phys.* **1986**, *85*, 2957.
(6) Ishikawa, M. *Macromolecules* **1979**, *12*, 502.
(7) Weisbuch, G.; Guéron, M. *J. Phys. Chem.* **1981**, *85*, 517.
(8) Granot, J. *Biopolymers* **1983**, *22*, 1831.
(9) Riedl, C.; Qian, C.; Savitsky, G. B.; Spencer, H. G.; Moss, W. F. *Macromolecules* **1989**, *22*, 3983.
(10) Škerjanc, J.; Dolar, D. *J. Chem. Phys.* **1989**, *91*, 6290.
(11) Rouzina, I.; Bloomfield, V. A. *J. Phys. Chem.* **1996**, *100*, 4292.
(12) Rouzina, I.; Bloomfield, V. A. *Biophys. Chem.* **1997**, *64*, 139.
(13) Le Bret, M.; Zimm, B. H. *Biopolymers* **1984**, *23*, 271.
(14) Murthy, C. S.; Bacquet, R. J.; Rossky, P. J. *J. Phys. Chem.* **1985**, *89*, 701.
(15) Paulsen, M. D.; Anderson, C. F.; Record, M. T., Jr. *Biopolymers* **1988**, *27*, 1249.
(16) Rouzina, I.; Bloomfield, V. A. *J. Phys. Chem.* **1996**, *100*, 4305.
(17) Bacquet, R. J.; Rossky, P. J. *J. Phys. Chem.* **1988**, *92*, 3604.
(18) Das, T.; Bratko, D.; Bhuiyan, L. B.; Outhwaite, C. W. *J. Chem. Phys.* **1997**, *107*, 9197.
(19) Lyubartsev, A. P.; Nordenskiöld, L. *J. Phys. Chem. B* **1997**, *101*, 4335.
(20) Pack, G. R.; Wong, L.; Lamm, G. *Biopolymers* **1999**, *49*, 575.
(21) Ni, H.; Anderson, C. F.; Record, M. T., Jr. *J. Phys. Chem. B* **1999**, *103*, 3489.
(22) Korolev, N.; Lyubartsev, A. P.; Rupprecht, A.; Nordenskiöld, L. *Biophys. J.* **1999**, *77*, 2736.
(23) Abascal, J. L. F.; Montoro, J. C. G. *J. Chem. Phys.* **2001**, *114*, 4277.
(24) Gregor, H. P.; Gregor, J. M. *J. Chem. Phys.* **1977**, *66*, 1934.